◆ Human Brain Mapping 32:1236–1249 (2011) ◆

Modulating Functional Connectivity Patterns and Topological Functional Organization of the Human Brain with Transcranial Direct Current Stimulation

Rafael Polanía*, **Michael A. Nitsche, and Walter Paulus**

Department of Clinical Neurophysiology, Georg-August University of Göttingen, 37075 Göttingen, Germany

Abstract: Transcranial direct current stimulation (tDCS) is a noninvasive brain stimulation technique that alters cortical excitability and activity in a polarity-dependent way. Stimulation for few minutes has been shown to induce plastic alterations of cortical excitability and to improve cognitive performance. These effects might be caused by stimulation-induced alterations of functional cortical network connectivity. We aimed to investigate the impact of tDCS on cortical network function through functional connectivity and graph theoretical analysis. Single recordings in healthy volunteers with 62 electroencephalography channels were acquired before and after 10 min of facilitatory anodal tDCS over the primary motor cortex (M1), combined with inhibitory cathodal tDCS of the contralateral frontopolar cortex, in resting state and during voluntary hand movements. Correlation matrices containing all 62 pairwise electrode combinations were calculated with the synchronization likelihood (SL) method and thresholded to construct undirected graphs for the θ, α, β, low-γ and high-γ frequency bands. SL matrices and undirected graphs were compared before and after tDCS. Functional connectivity patterns significantly increased within premotor, motor, and sensorimotor areas of the stimulated hemisphere during motor activity in the 60–90 Hz frequency range. Additionally, tDCS-induced significant intrahemispheric and interhemispheric connectivity changes in all the studied frequency bands. In summary, we show for the first time evidence for tDCS-induced changes in brain synchronization and topological functional organization. *Hum Brain Mapp 32:1236–1249, 2011.*

Key words: cortical excitability; EEG; graph; synchronization; tDCS

INTRODUCTION

Transcranial direct current stimulation (tDCS) is a noninvasive brain stimulation tool that alters cortical excitability and activity via application of weak direct currents. The respective excitability alterations—enhancement by anodal and reduction by cathodal tDCS—can last for over an hour after the end of stimulation [Nitsche and Paulus, 2001; Nitsche et al., 2003b]. The after-effects of tDCS are NMDA receptor–dependent [Nitsche et al., 2003a, 2004], and thus share some similarities with long-term potentiation and depression, which are thought to be the neurophysiological derivates of learning and memory formation. Consequently, anodal tDCS of the primary motor cortex

Additional Supporting Information may be found in the online version of this article.

Contract grant sponsor: Rose Foundation.

*Correspondence to: Rafael Polanía, Department of Clinical Neurophysiology, Georg-August University of Göttingen, Robert Koch Str 40, 37075 Göttingen, Germany.
E-mail: rafael.polania@med.uni-goettingen.de

Received for publication 30 January 2010; Revised 27 April 2010; Accepted 7 May 2010

DOI: 10.1002/hbm.21104
Published online 6 July 2010 in Wiley Online Library (wileyonlinelibrary.com).

has been shown to improve motor learning [Nitsche et al., 2003c], visual–motor coordination [Antal et al., 2004], motor training effects, and nondominant hand function in healthy humans [Boggio et al., 2006]. One important aspect of the beneficial effect of tDCS on these parameters might be a strengthening of learning-related synaptic connections. Hereby tDCS might improve the functional connectivity between segregated cortical areas involved in the task under study. However, the effect of tDCS on functional connectivity itself has so far not been explored.

The human cerebral cortex exhibits specific functional interconnection patterns linking the whole brain regions (between cell populations and individual cortical neurons) [Salin and Bullier, 1995]. Further analysis has demonstrated that such patterns are neither completely regular nor completely random, i.e., the human brain integrates both localized and segregated information processing [Sporns et al., 2004]. Functional connectivity of the human brain is defined as the temporal dependence of neuronal activity across different brain regions. Coherence has been widely used in electroencephalography (EEG) analysis to investigate functional connectivity, and it has been demonstrated that oscillatory activity is correlated between cortical regions that participate in the same functional network, e.g., for visual and motor networks [Cordes et al., 2000; Fox and Raichle, 2007]. However, this approach is not sensitive to nonlinear dynamic interdependencies [Breakspear et al., 2003] and recent studies have reported significant nonlinear interdependencies of the EEG signals [Stam, 2005; Stam and Reijneveld, 2007]. Hence, in the present study, we use a recently introduced method called synchronization likelihood (SL) that measures both linear and nonlinear interdependencies between dynamical systems [Stam and Dijk, 2002].

Characterization of complex human brain networks has been of increasing interest in the recent years using graph theory as a mathematical approach [Micheloyannis et al., 2006; Sporns and Zwi, 2004; Stam et al., 2007, 2009]. A graph is defined as a mathematical representation of a network consisting of a set of elements (nodes) and a set of connections (edges) that interconnect the nodes of the graph. In our study, each node is represented by an EEG electrode and the edges represent functionally connected brain regions that are calculated with SL. This approach allows to examine the functional connectivity architecture of the brain, which might provide information regarding its organization linked to the capability of integration and transference of information within and between different regions. Consequently, the results of recent studies suggest that cognitive dysfunction in Alzheimer's disease (AD) could be at least partly explained by a functional disconnection between distant brain areas. Here a disruption of functional connectivity when compared with healthy subjects was reported when building functional networks from EEG data [Stam et al., 2007]. Interestingly, anodal tDCS enhances the performance of memory tasks in AD [Boggio et al., 2009]. Therefore, it might be speculated that tDCS affects functional cortical connectivity. Hence, tDCS and graph theoretical analysis may be combined to achieve a better insight on the impact of tDCS on cortical functions.

Recent studies have demonstrated that movement-related processing results in the modulation of neural synchronization over α (8–12 Hz) and β (13–30 Hz) bands. Neural synchronization at these frequency bands has been suggested to be of importance for cortico-cortical and cortico-subcortical motor processing [Klostermann et al., 2007]. Further studies have shown intrinsic $\sim$10 Hz rhythmic oscillations in motor cortex slices [Castro-Alamancos and Rigas, 2002] and in vivo [Castro-Alamancos et al., 2007]. Regarding high-frequency oscillations, increased γ activity during maintained isometric contraction was localized in the hand motor cortex using a MEG source modeling approach [Tecchio et al., 2008], and Waldert et al. [2008] reported an increased power in the 60–85 Hz frequency band in MEG recordings over the contralateral sensorimotor cortex. Cheyne et al. [2008] identified 65–80 Hz oscillations in the primary motor cortex that originated from self-paced hand movements, which were found to be effector-specific, possibly reflecting the activation of cortico-subcortical networks involved in feedback control of simple movements. Given that previous tDCS studies have demonstrated that cortical stimulation facilitates motor functions in humans, it is of great interest to investigate how excitatory anodal tDCS over the motor cortex might affect the synchronization of such brain oscillations belonging to cortical networks involved in the performance of motor tasks.

In the present study, we aim to investigate whether tDCS-generated excitability changes induce modifications of functional cortical architecture in humans. To achieve this, we used a graph theoretical analysis based on 62-channel EEG recordings in healthy volunteers before and after bipolar tDCS—anode over M1 and cathode over contralateral orbit—during resting state and the performance of a simple motor task. Offline, EEGs were filtered to the θ, α, β, low-γ (30–60 Hz), and high-γ (60–90 Hz) frequency bands. Correlation matrices were based on the calculation of the SL between all pairwise combinations of the 62 EEG channels and subsequently undirected graphs were built for each frequency band. SL matrices and undirected graphs were compared before and after tDCS.

MATERIALS AND METHODS

Subjects

The study involved 10 healthy volunteers (six women and four men; mean age, 26 $\pm$ 4 years; age range 21–32 years). Subjects were informed about all aspects of the experiments and all gave informed consent. None of them suffered from any neurological or psychiatric disorder, had metallic implants/implanted electric devices, or took any medication regularly, and none of them took any

medication in the 2 weeks before their participation in any of the experiments. All subjects were right handed, according to the Edinburgh handedness inventory [Oldfield, 1971]. The experiments conform to the Declaration of Helsinki and were approved by the Ethics Committee of the University of Göttingen.

Transcranial Direct Current Stimulation

Bipolar stimulation was delivered by a battery-driven electrical stimulator (NeuroConn GmbH, Ilmenau, Germany) through a pair of square rubber electrodes (4×4 cm^2), placing the anode over the left M1 and the cathode over the contralateral orbit. The rationale for stimulating the dominant hemisphere is that externally induced excitability alterations by tDCS have been predominantly evaluated by neurophysiological techniques at the left motor cortex in right-handers—using it as a model [Nitsche and Paulus, 2000, 2001], therefore, it would be appropriate to keep it as a reference. Moreover, functional connectivity of the dominant hemisphere—in terms of greater synchronization—might be expected to be larger than that of nondominant one [Amunts et al., 2000]. To properly position the electrode over the left M1, the representational field of the right hand was determined using single pulse transcranial magnetic stimulation (TMS). The electrodes were fixed under the EEG cap—only during stimulation—using elastic bands. tDCS was applied for 10 min with a current strength of 1 mA. Subjects sat awake in a comfortable reclined chair during the stimulation. For the sham stimulation sessions, the current was applied for 30 s at the beginning of the stimulation and then turned down. Stimulation electrodes were removed during EEG recordings. Subjects were blinded for stimulation conditions.

Electroencephalography

EEGs were recorded against an average reference electrode (EEG-ANT system) at the following 62 positions of the international 10–20 system: Fp1, Fpz, Fp2, F7, F3, Fz, F4, F8, FC5, FC1, FC2, FC6, T7, C3, Cz, C4, T8, CP5, CP1, CP2, CP6, P7, P3, Pz, P4, P8, Poz, O1, Oz, O2, AF7, AF3, AF4, AF8, F5, F1, F2, F6, FC3, Fcz, FC4, C5, C1, C2, C6, CP3, Cpz, CP4, P5, P1, P2, P6, PO5, PO3, PO4, PO6, FT7, FT8, TP7, TP8, PO7, and PO8. Electrode impedance was monitored throughout the experiment to be less than 5 kΩ during both before and after the end of the tDCS. Sample frequency was 1,024 Hz at an analogue-digital precision of 24 bits. EEGs were recorded in a sound-attenuated room where subjects sat in a comfortable reclined chair. The EEG cap setup took between 20 and 30 min for all sessions—during this time subjects were sitting in the reclined chair. Subjects participated in two sessions, tDCS and sham stimulation, respectively, separated by at least 8 days. Twenty-second EEG epochs were acquired immediately before and after 10 min of tDCS for resting state (open eyes, free of eye blinking) and motor task performance, respectively. For the motor task, during the 20 s epoch subjects were asked to move the index finger to the thumb of the right hand during the whole 20 s at subject's maximum own speed. The order of real and sham tDCS sessions was randomized between subjects. Rest and motor task conditions were not randomized. The reason behind this was to avoid an influence of task performance on functional connectivity in the subsequent rest condition. Therefore, the rest condition was always performed before the motor task. The epochs were down-sampled to 540 Hz, resulting in time series of 10,800 samples. This resulting number of samples is large enough to calculate the SL between two times series. The exact procedure will be described in the following subsection.

Synchronization Likelihood

Correlations between all pairwise combinations of the 62 EEG channels were computed with the SL, which has been used in several previous studies [Micheloyannis et al., 2006; Stam et al., 2007, 2009]. Here we give a brief description of the calculation. The SL is a measure of the generalized synchronization of two dynamical systems X and Y that is sensitive to linear and nonlinear interdependencies. The first step is to convert the time series: $x_1, x_2, \ldots x_N$; into a set of m-dimensional vectors whose components are the time-delayed values of the variables:

$$X_i = (x_1, x_{i+T}, x_{i+2\times T}, x_{i+3\times T}, \ldots, x_{i+(m-1)\times T}), \quad X_i \in \mathrm{R}^m$$

where T is the time lag. Thus, the information in the one-dimensional data has been converted to a set of m-dimensional patterns, where $\hat{N} = N - (m \times T)$ vectors (patterns) can be reconstructed. The correlation integral $C(r, \hat{N})$ is the likelihood that two randomly chosen vectors will be closer than a cut-off distance r_x:

$$C(r_x, \hat{N}) = \frac{2}{\hat{N}(\hat{N} - w)} \sum_{i=1}^{\hat{N}} \sum_{j=i+w}^{\hat{N}-w} H(r_x - |X_i - X_j|),$$

where $H(x)$ is the Heaviside step function and w is the Theiler correction for autocorrelation [Theiler, 1986]. The vertical bars represent the Euclidean distance between the vectors. Before defining the SL, we find r_x and r_y by setting a correlation reference $P_{ref} = C(\hat{N}, r_x) = C(\hat{N}, r_y)$. Now the SL between X and Y is defined as:

$$SL_{xy} = \frac{2}{\hat{N}(\hat{N} - w)P_{\mathrm{ref}}} \sum_{i=1}^{\hat{N}} \sum_{j=i+w}^{\hat{N}-w} \times H(r_x - |X_i - X_j|)H(r_y - |Y_i - Y_j|),$$

which is the conditional likelihood that the distance between Y_i and Y_j will be smaller than a cut-off distance r_y,

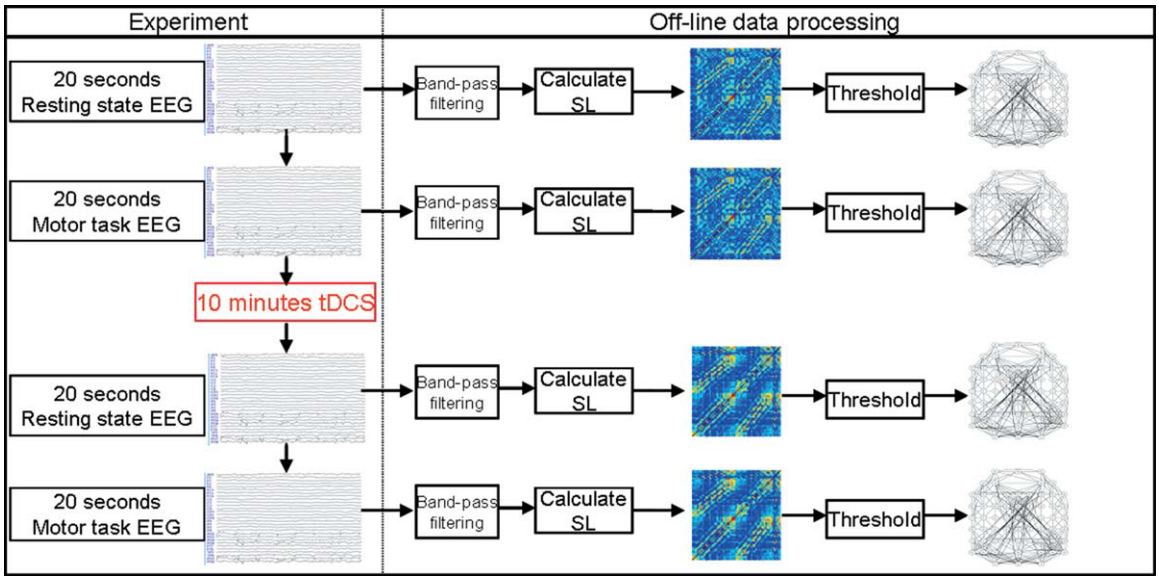

Figure 1.

Experimental and data processing flow. The left column shows the experimental steps performed on each subject. First, 20-s epochs were recorded during rest and the performance of the motor task. Afterwards, the stimulation electrodes were placed over the scalp—under the EEG cap—and tDCS was applied for 10 min. Immediately after the stimulation, the electrodes were removed and again 20-s epochs were recorded during rest and the performance of the same motor task (strictly in the same order for all the subjects either for the real and sham tDCS sessions). The recorded epochs were processed offline. First, the epochs were band pass filtered, then the SL was calculated and subsequently a SL matrix was built. Finally, the SL matrices were thresholded and then undirected graphs were built.

given that the distance between X_i and X_j is smaller than a cut-off distance r_x . Notice that in case of complete synchronization $SL_{xy} = 1$ and in case of complete independence $SL_{xy} = P_{ref}$. A recent study has developed a framework to optimize the parameters T and m, by using prior knowledge of the frequency bands of interest [Montez et al., 2006]. Therefore, in the present study, the following parameters T and m were used for each frequency band: θ: $T = 22$, $m = 7$; α: $T = 15$, $m = 6$; β: $T = 6$, $m = 9$; low γ: $T = 3$, $m = 7$; high γ: $T = 2$, $m = 6$. Finally for the calculation of the SL, P_{ref} was set to 0.02 for all frequency bands.

Undirected Graphs

The SL is calculated for all possible pairwise combinations, resulting in a $N \times N$ ($N = 62$ EEG channels) matrix, where each entry N_{ij} contains SL_{ij}. Then, for each individual data set, a connectivity graph G was formed consisting of N nodes (EEG channels) and a set of undirected edges E (functional connectivity) by applying a correlation threshold T to the SL matrix:

$$e_{ij} = \begin{cases} 1 & \text{if } N_{ij} > T \\ 0 & \text{otherwise} \end{cases}$$

Hence, if the SL value between a pair of brain regions i and j is greater than the given value T, an edge is said to exist. When setting a threshold T, the number of edges—functional connections—can be quantified per node and afterward averaged, resulting in a graph parameter called the mean connectivity degree K. Figure 1 shows the experimental flow diagram performed on each subject during the EEG-tDCS sessions and the posterior off-line data preprocessing.

Data Processing and Statistical Analysis

EEGs were band-pass filtered at the θ, α, β, low-γ (30–60), and high-γ (60–90) frequency bands. SL matrices were built from the filtered EEG epochs before and after tDCS. Then we compared the functional connectivity patterns obtained in the SL matrices before and after stimulation. Functional synchronization between two EEG electrodes was defined to be significantly different if the following criteria were met: (1) using a paired two-tailed t-test, for each SL_{ij} between the two groups (i.e., before and after stimulation) at the threshold of $p < 0.01$ uncorrected and (2) SL values of those connectivities were significantly different from zero at $p < 0.01$ using a one-sample two-tailed t-test in at least one group. Hence, the functional connections that met the previous conditions were quantified and mapped—i.e., EEG channels that became significantly synchronized (or desynchronized) after tDCS. The following "contrasts" were analyzed: (1) Task before

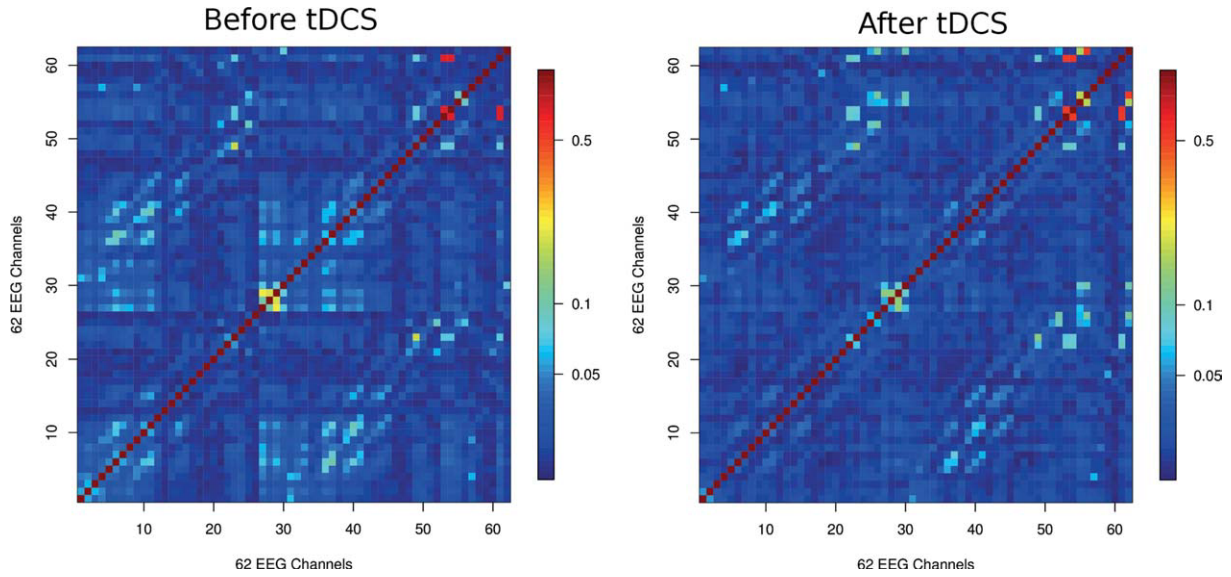

Figure 2.

Mean SL matrices for all subjects in the 60–90 Hz γ band during the performance of the motor task before (left) and after (right) tDCS. The scale on the right side of the figures shows the SL value in logarithmic scale. The order of the electrodes from 1 to 62 is: Fp1, Fpz, Fp2, F7, F3, Fz, F4, F8, FC5, FC1, FC2, FC6, T7, C3, Cz, C4, T8, CP5, CP1, CP2, CP6, P7, P3, Pz, P4, P8, Poz, O1, Oz, O2, AF7, AF3, AF4, AF8, F5, F1, F2, F6, FC3, Fcz, FC4, C5, C1, C2, C6, CP3, Cpz, CP4, P5, P1, P2, P6, PO5, PO3, PO4, PO6, FT7, FT8, TP7, TP8, PO7, and PO8.

stimulation—rest before stimulation; (2) task after stimulation—rest before stimulation; (3) rest after stimulation—rest before stimulation, and (4) task after stimulation—task before stimulation.

All computations performed in this study were done off-line by in-house software written by one of the authors (RP) fully developed under both R [Team, 2009] and C++ compiled using gcc version 4.3.2 under Linux i386.

RESULTS

SL Matrices

The first step after band-pass filtering is the calculation of the SL matrices. Figure 2 shows an example of the obtained SL matrices ($N \times N, N = 62$) for the high-frequency γ band (60–90 Hz) during performance of the motor task before and after anodal tDCS, because this is the frequency band and condition at which the most prominent results were obtained after the complete analysis. Light-blue to red regions indicate high levels of synchronization among the 62 electrodes. Figure S1 (see Supporting Information) shows the respective SL matrices for the θ to low-γ frequency bands.

The functional connections that became significantly (de)synchronized after tDCS were identified by the direct comparisons of all possible pairwise combinations as described in the methods section (data processing and statistical analysis subsection). Figure 3 shows exactly where such significant strengthened/weakened functional connections are located for the studied contrasts. When comparing the effects of tDCS on motor task performance with the resting state condition (first two columns in Fig. 3), a clear modulation can be observed in the θ (modulation in the whole brain, but mainly in the left hemisphere), α (modulation on left motor, parietal and contralateral frontal areas), and high-γ bands (modulation mainly within the whole left hemisphere). The effects of tDCS on resting state network connectivity are displayed in the third column of Figure 3. Here, the major impact occurred at the θ, α, and β bands with a marked increase in synchronization within frontal areas. Lastly, the effects of tDCS in the dynamically active brain—during the performance of a motor task—can be observed in the fourth column of Figure 3. Here, for the θ and α bands, synchronization significantly increased within parieto-occipial and frontal regions of the left hemisphere (hemisphere where anodal stimulation was applied over the motor cortex). β and low-γ bands did not show any significant change, while the most prominent result was found for the high-γ frequency band. At this frequency, the comparison of the SL matrices between before-real-stimulation and after-real-stimulation (Fig. 4a) show similar patterns as the comparison between after-sham-stimulation and after-real-stimulation (Fig. 4b), with a slight reduction in the number of significant connections in Figure 4b with respect to Fig. 4a. A significant increase of synchronization can be observed within regions over

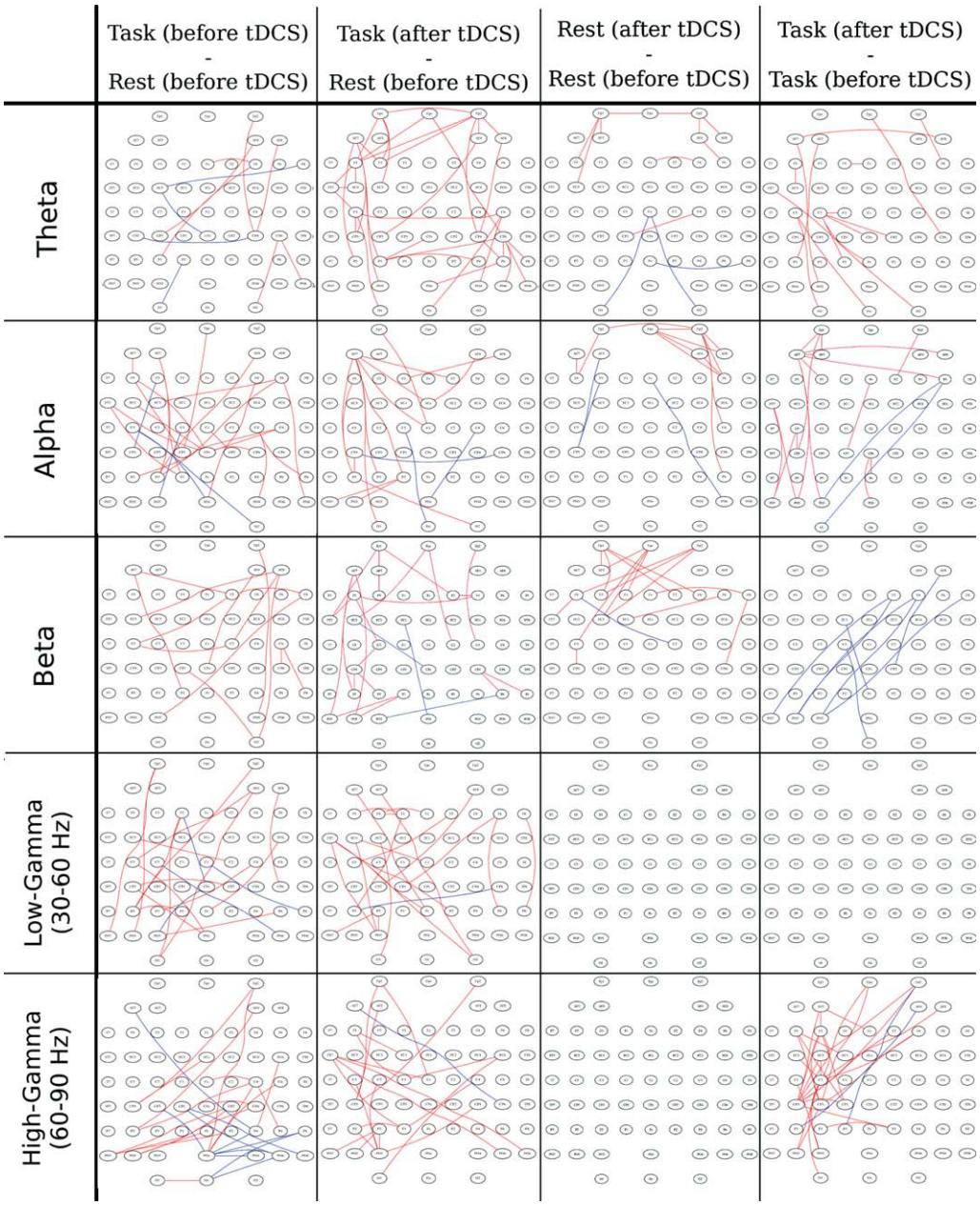

Figure 3.

EEG channels which became significantly synchronized (red) and desynchronized (blue) according to the threshold parameters described in the methods section (Data processing and statistical analysis subsection). Columns from left to right show the following contrasts: (1) Task before stimulation—rest before stimulation; (2) task after stimulation—rest before stimulation; (3) rest after stimulation—rest before stimulation; and (4) task after stimulation—task before stimulation.

the left premotor, motor, and sensorimotor areas. Additionally, few connections linking ipsi- or contra-lateral frontal electrodes with motor areas occur. On the other hand, a significant interhemispheric desynchronization (blue connections in Fig. 4) appears between left parieto-occipital and right frontal electrodes in the α, β, and high-γ frequency bands. Before and after sham stimulation, we can see that no significant changes emerged (Fig. 4c), except for a few number of desynchronized channels in the left parietal region.

Regarding the effects of tDCS over resting state networks, in the third column of Figure 3, a synchronization

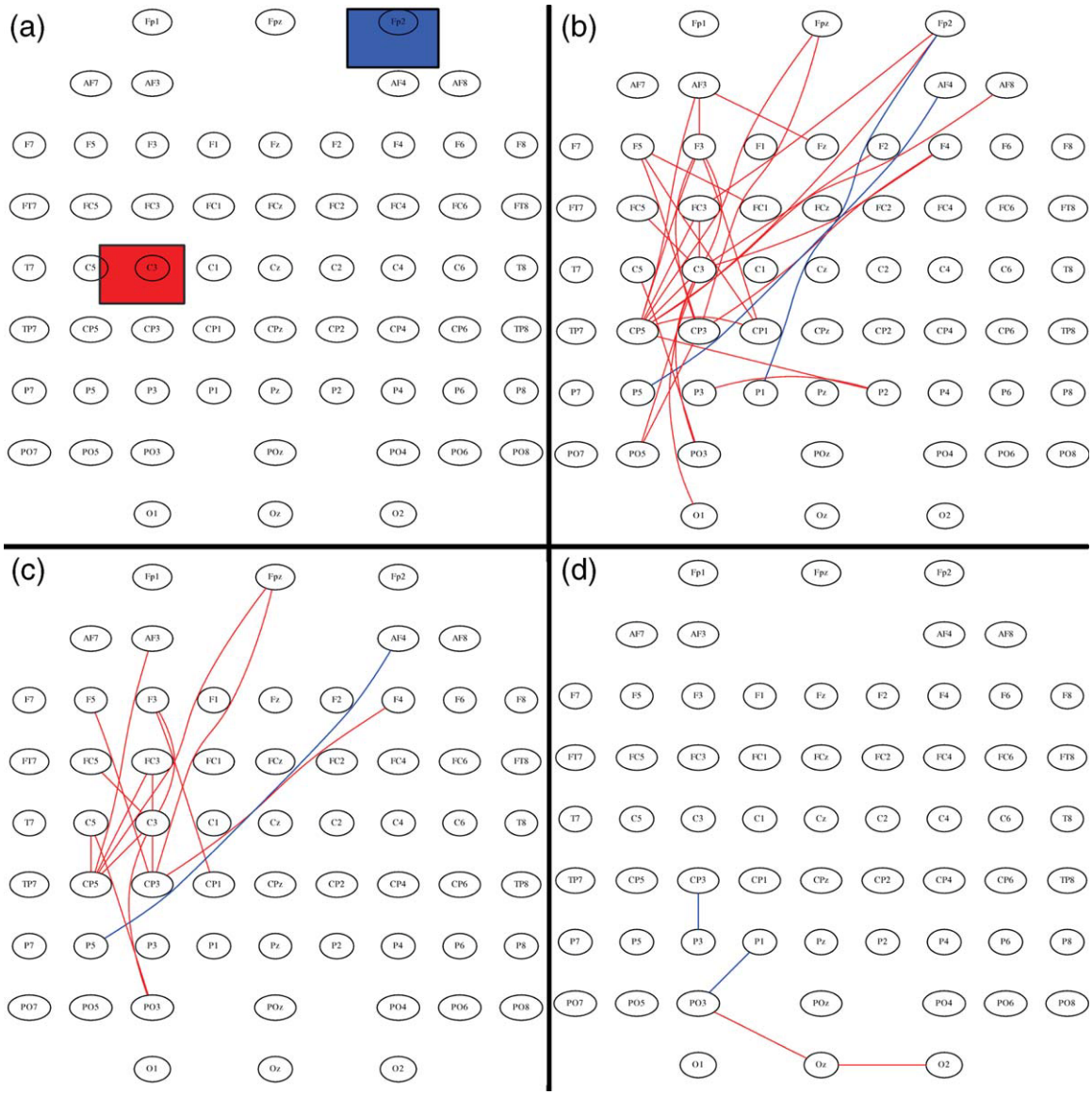

Figure 4.

EEG channels which became significantly synchronized (red) and desynchronized (blue) according to the threshold parameters described in the methods section (Data processing and statistical analysis subsection) during the motor task condition at the high-γ frequency band. The compared experimental conditions are: (**a**) Location of the anodal (red) and cathodal (blue) tDCS electrodes during the 10 min of stimulation. (**b**) Before-real-stimulation and after-real-stimulation. (**c**) After-sham-stimulation and After-real-stimulation. (**d**) Before-sham-stimulation and After-sham-stimulation.

increase mainly within frontal electrodes at the relatively low frequency bands—θ, α, and β bands is apparent.

The analysis of the contrasts of connectivity before and after the sham stimulation did show no relevant changes of functional connectivity (Fig. S2, Supporting Information), thus validating the results on the effects of tDCS. The results displayed in Figures 3 and 4 show where the pairs of EEG channels became significantly (de)synchronized; however, it does not deliver information about the effects of tDCS on the functional topological organization linking the whole brain. To achieve this, SL matrices were converted to undirected graphs.

Undirected Graphs

Undirected graphs were built before and after tDCS by setting a threshold T to the corresponding SL matrices. For

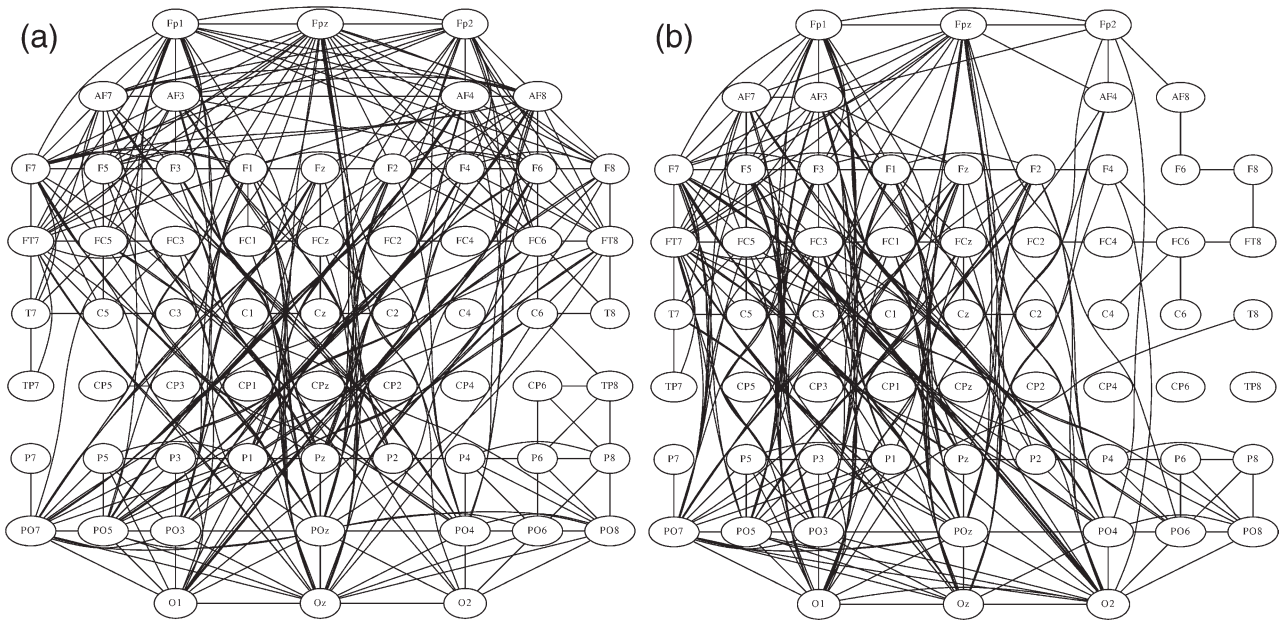

Figure 5.

SL matrices of Fig. 2 were converted to undirected graphs by setting the mean connectivity degree threshold to $K = 10$. (**a**) Before real tDCS. (**b**) After real tDCS. After tDCS the functional connections increased in the left hemisphere.

values of $T = P_{ref}$, we expect the corresponding graphs to be fully connected and having a mean connectivity degree $K = 62$. Increasing the threshold will eliminate weaker connections, resulting in graphs with a reduced number of edges. However, if we compare graphs setting the same threshold for all the subjects, the mean connectivity degree K might differ across the respective resulting graphs. To control for this effect, we built and compared undirected graphs having the same connectivity degree K, i.e., we assure that the number of connections in all the graphs is the same. Therefore, all the SL matrices were thresholded up starting at $T = P_{ref}$ until the mean connectivity degree $K = 10$. The reason to choose this value for K was that we assured the graphs for all subjects to be fully connected, i.e., we assured that none of the graphs were divided into two or more subgraphs (fragmentation). The mean SL matrices shown in Figure 2 were converted to graphs using $K = 10$ (Fig. 5). These undirected graphs represent the functional connections linking the whole brain in the 60–90 Hz γ band during the performance of a motor task. By simple inspection it can be seen that after tDCS, the functional connections increased in the left hemisphere, thus, matching the change in the connectivity pattern shown in Figure 4 (consider that both Fig. 5a,b have the same number of edges).

Regarding the resting networks, we built undirected graphs for the β band before and after tDCS—setting $K = 10$ as well—which was one of the relatively lower bands were we observed synchronizations within the frontal region induced by tDCS. In Figure 6, it can be observed that after tDCS at frontal electrodes FPz, FP2, AF4, AF8, and F8 the number of connections increased (once more consider that both Fig. 6a,b have the same number of edges).

To obtain a picture of where the functional changes occurred in the brain after stimulation during performance of the motor task, the number of left and right intrahemispheric, as well as the interhemispheric, connections were quantified before and after tDCS setting the mean connectivity degree $K = 10$. Table I and Figure 7 show that after stimulation the number of connections within the left hemisphere significantly increased for the θ, α, and β bands; the number of interhemispheric connections decreased significantly in the θ, α, and high-γ band, while the number of right intrahemispheric connections remained without significant changes for all of the analyzed frequency bands. The effect of tDCS on this analysis is further confirmed by the comparison between before-sham and after-sham, where no significant differences where found for all of the analyzed frequency bands.

As the threshold T for the construction of the undirected graphs was variable, Table II shows the mean $\pm$ SD of T when setting $K = 10$ for all the frequency bands, before and after tDCS for the rest and motor task conditions.

DISCUSSION

In the present study, we used EEG recordings during the performance of voluntary hand movements to evaluate

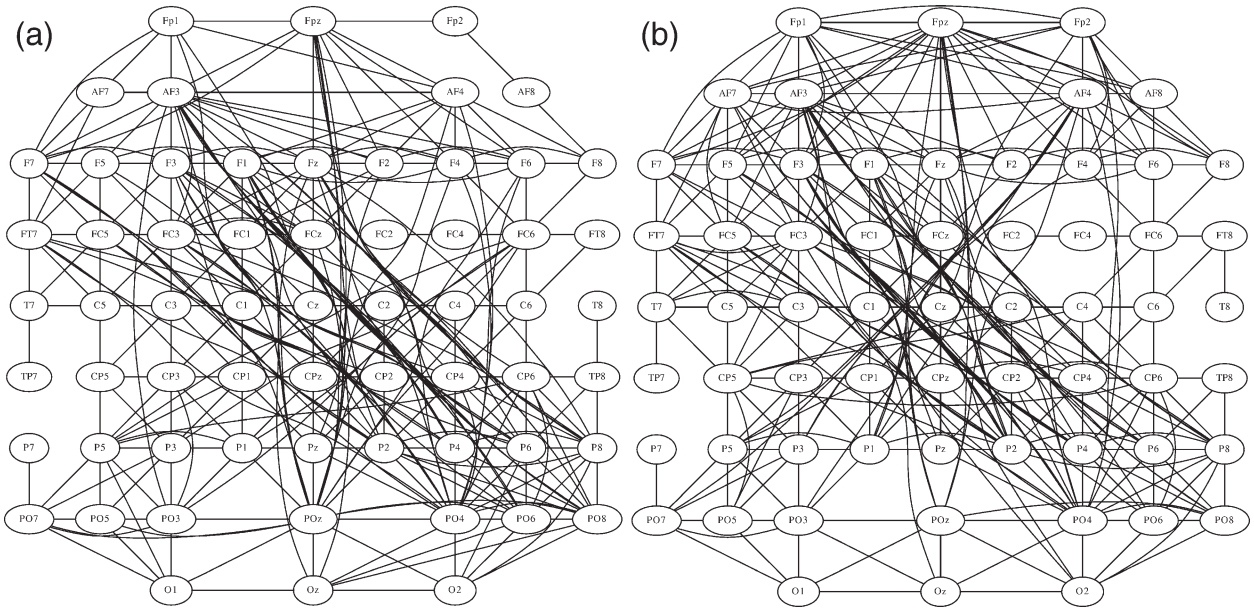

Figure 6.

SL matrices in the resting state condition at the β frequency band were converted to undirected graphs by setting the mean connectivity degree threshold to $K = 10$. (**a**) Before real tDCS. (**b**) After real tDCS. After tDCS the functional connections increased over right frontal electrodes - AF4, AF8, FP2, and FPz.

functional cortical network alterations induced by excitatory anodal tDCS over the primary motor cortex. When we evaluated the effects of tDCS in the dynamic brain, we found that at relatively lower frequency bands an increase of synchronization occurred mainly within frontal and parieto-occipital electrodes, especially in the θ and α band (Fig. 3, fourth column). It has been demonstrated that θ and α rhythms originate in calcarine, occipito-parietal, and somato-sensory cortices, which are modulated by sensory input and motor output through complex cortico-cortical and thalamo-cortical interactions [Hari et al., 1997; Manshanden et al., 2002; Steriade et al., 1990]. The increase in synchronization between these areas does not appear after placebo stimulation, therefore, suggesting to be enhanced by tDCS (Fig. S2, Supporting Information). Nevertheless, it should be considered that EEG recordings collected few days apart might lead to differences in baseline measurements, thus, generating some variability in the reproducibility of the EEG measurements—e.g., notice the slight difference between column 1 of Figure 3 and Supporting Information Figure S2, which show task-rest comparisons before any intervention of either real tDCS and sham stimulation. Although the patterns are similar, a slight increase in the number of connections—in the β and high-γ bands—in the sham session with respect to the real tDCS session can be noticed. This minor difference can however

TABLE I. Paired *t*-test for the total number of inter- and intrahemispheric connections, setting $K = 10$ for the undirected graphs[a]

	After tDCS: before tDCS			After tDCS: after sham			After sham: before sham		
Frequency	Interhemisph	Intraleft	Intraright	Interhemisph	Intraleft	Intraright	Interhemisph	Intraleft	Intraright
θ	0.1	(↑) 0.005	0.71	0.19	(↑) 0.015	0.6	0.56	0.45	0.25
α	(↓) 0.04	(↑) 0.01	0.2	0.08	(↑) 0.03	0.45	0.71	0.57	0.75
β	0.3	(↑) 0.004	0.85	0.25	(↑) 0.02	0.89	0.22	0.5	0.89
Low-γ	0.4	0.33	0.3	0.35	0.64	0.76	0.39	0.44	0.68
High-γ	(↓) 0.05	(↑) 0.04	0.9	0.11	(↑) 0.05	0.8	0.31	0.34	0.92

Paired *t*-test, $n = 10$, degrees of freedom = 9.

[a]Arrows indicate where the number of inter- and intrahemispheric connections significantly ($P < 0.05$) increased (↑) or decreased (↓).

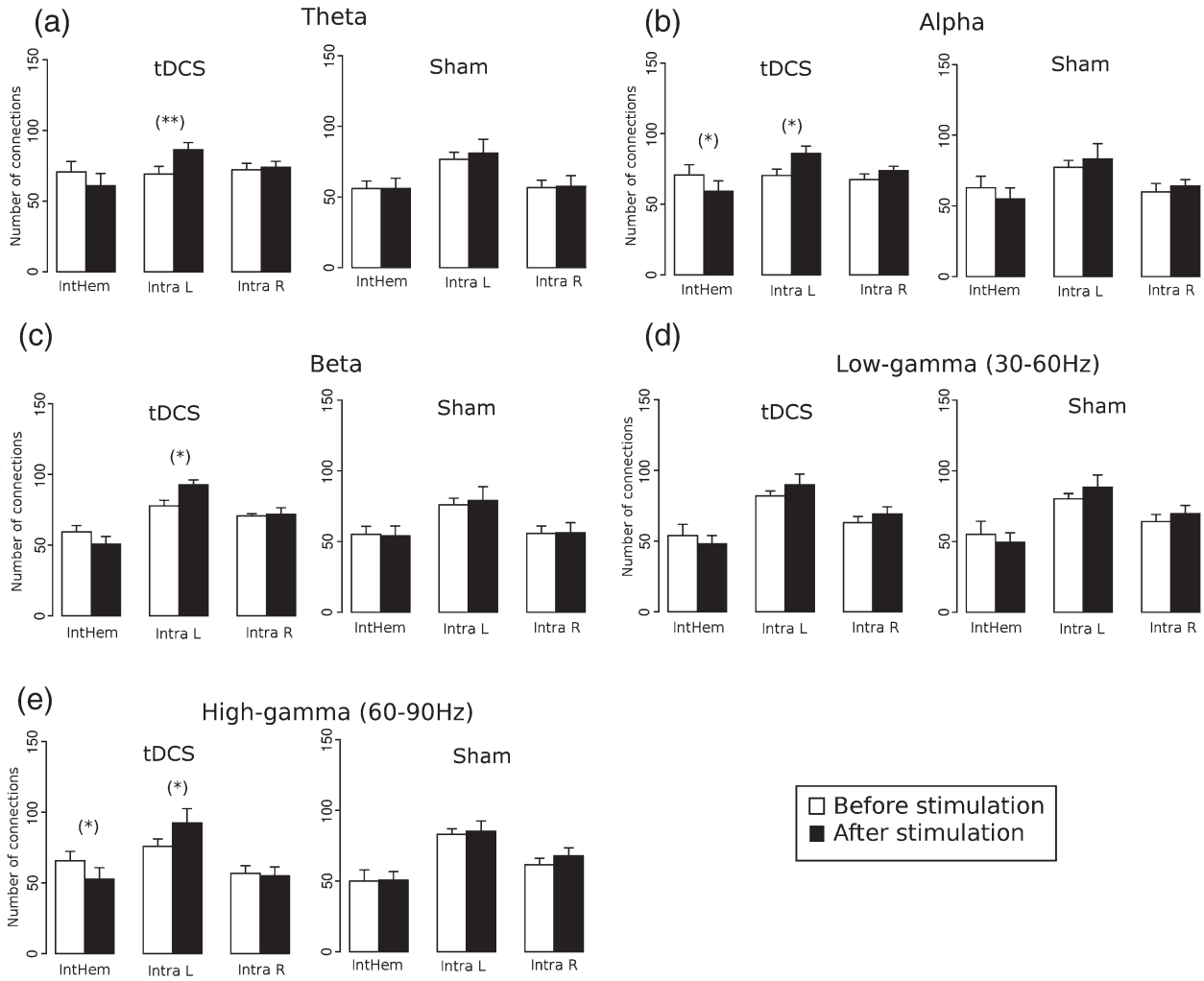

Figure 7.

Number of inter- (intHem) and intra-hemispheric [intra-hemispheric left (intra L) and right (intra R)] connections before (white) and after (black) real tDCS and sham stimulation during the performance of the motor task when setting the mean connectivity degree threshold $K = 10$ in the θ (**a**), α (**b**), β (**c**), low-γ, (**d**) and high-γ (**e**) frequency bands (mean ± SEM). Black asterisk indicates where the difference between the two groups is significant (paired *t*-test: (*) $P < 0.05$; **$P < 0.01$).

TABLE II. Mean values and paired *t*-test of threshold *T*, when setting $K = 10$

	Resting state			Motor task		
Frequency	mean $T \pm$ SD. before tDCS	mean $T \pm$ SD after tDCS	Paired *t*-test $n = 10$,df=9	mean $T \pm$ S.D. before tDCS	mean $T \pm$ SD after tDCS	Paired *t*-test $n = 10$,df = 9
θ	0.052 ± 0.009	0.056 ± 0.01	0.43	0.051 ± 0.002	0.068 ± 0.008	0.08
θ	0.048 ± 0.01	0.049 ± 0.007	0.79	0.053 ± 0.01	0.061 ± 0.01	0.075
B	0.043 ± 0.008	0.056 ± 0.007	0.17	0.045 ± 0.006	0.049 ± 0.009	0.15
Low-γ	0.035 ± 0.005	0.037 ± 0.005	0.32	0.034 ± 0.005	0.04 ± 0.008	0.13
High-γ	0.03 ± 0.004	0.031 ± 0.005	0.55	0.031 ± 0.006	0.042 ± 0.009	0.1

not explain the major alterations caused by the combination of tDCS and task performance on functional connectivity. On the other hand, a prominent increase in synchronization of regions involved in motor task performance was found in the high-γ (60–90 Hz) frequency band (Fig. 3 fourth column and Fig. 4). Here, EEG electrodes around C3 and C5 turned out to be highly synchronized after tDCS during performance of the motor task, regions that belong to the cortical regions where excitatory anodal stimulation was applied (such increase in synchronization is not observed after placebo stimulation). Oscillations (60–90 Hz) have been demonstrated to accompany motor and sensorimotor processes in the human brain [Omlor et al., 2007; Schoffelen et al., 2005]. Moreover, recent studies have demonstrated that voluntary hand movements elicit high-frequency γ oscillations (>60 Hz) over sensorimotor areas. Recordings with intracerebral depth electrodes and electrocorticogram (ECoG) have confirmed movement-related increases of high γ bands in motor and premotor areas [Brovelli et al., 2005]. Noninvasive studies in humans have also demonstrated the presence of movement-related high γ oscillations. Increased γ activity during maintained isometric contraction was localized in the hand motor cortex using a MEG source modeling approach [Tecchio et al., 2008], and Waldert et al. [2008] report an increased power of the 60–85 Hz frequency band in MEG recordings over the contralateral sensorimotor cortex. When comparing the SL matrices before and after stimulation at the high-γ frequency band (60–90 Hz) during the performance of a motor task (Fig. 4), we found that tDCS has an impact on motor task-related functional network synchronization not only within the stimulated motor area but also involving synchronization within premotor and sensorimotor areas. Thus, the excitability increase induced by anodal stimulation [Nitsche and Paulus, 2000, 2001] might be related to the functional connectivity increase between cortical areas involved in the performance of a motor task, furthermore, showing to be frequency and topographic specific. Moreover, task performance alone results in a qualitatively different pattern of synchronization, thus tDCS might not only enhance synchronization but also can change the pattern of task-related activation, possibly uncovering a beforehand subliminal activation—notice the difference between the first and second column of Figure 3 (where the effects of tDCS where evaluated by comparing task against rest) and then compare the second column with the fourth column of the same figure (where the effects of tDCS where evaluated in task performance only). It might be that this tDCS-related increase of functional synchronization is relevant for the beneficial effects of anodal tDCS on motor learning [Nitsche et al., 2003c], motor training effects, and nondominant hand function in humans [Boggio et al., 2006]. Even though the motor task performed by the subjects in the present study was rather simple—subjects were asked to perform finger tapping at maximum speed—attention and sensory feedback was needed, thus, requiring the participation of premotor and sensorimotor regions together with the primary motor cortex—regions that appeared to be significantly synchronized after tDCS in the high-γ frequency range. Hence, we hypothesize that an important aspect of the beneficial effect of excitatory anodal tDCS might be that it enhances strengthening of dynamical task-related synaptic connections. These strengthened connections over the anodal-stimulated hemisphere are moreover specifically related to changes in the topological functional organization of the whole brain in the high-frequency γ-band (Figs. 5 and 7e). The increase of connectivity in the stimulated hemisphere is balanced by a decrease on the interhemispheric connections while the right hemisphere remained more or less unchanged. The same tendency was observed in all the other studied frequency bands (Table I and Fig. 7). Moreover, in Table II, it is interesting to see that the threshold T—when setting $K = 10$—was close to significantly increased after tDCS intervention for all the studied frequency bands during the motor task performance. On the other hand, notice that T remained more or less constant after tDCS for the resting condition. Thus, it might be speculated that functional connectivity in the whole dynamic brain is shifted and modulated by the effects of combined motor activity and excitatory transcranial stimulation.

In addition, in the high-frequency band, tDCS induced some significant desynchronizations between left parieto-occipital regions and contralateral frontal electrodes. When comparing the SL matrices before and after sham stimulation such changes are not present, suggesting that these desynchronizations are tDCS-related (Figs. 4 and S2). This result can be explained by the fact that subjects were asked to perform the finger tapping task at their own maximum speed, therefore, requiring concentration and visual attention to perform a motor-coordinated task. Recent studies have demonstrated that noninvasive cortical stimulation enhances performance of visuo-motor and motor coordination processing in healthy humans [Antal et al., 2004]. Indeed, in Figure 4a,b, it can be noticed that some parieto-occipital and contralateral frontal regions significantly increased the functional coupling with motor related areas. Therefore, the excitatory changes induced by tDCS over M1 might strengthen functional connections linking motor related areas with motor-coordination areas, thus, diminishing occipital frontal coupling and increasing motor-related synchrony. In accordance, Cheyne et al., [2008] identified high-frequency γ oscillations in motor areas that originated from self-paced hand movements, which were found to be effector specific, possibly reflecting the activation of cortico-subcortical networks involved in feedback control of simple movements. Moreover, previous studies support the idea that tDCS affects not only the underlying cortico-spinal excitability but also distant neural networks, producing widespread changes in other regions of the brain [Boros et al., 2008; Lang et al., 2005; Vines et al., 2008]. EEG studies show that stimulation over a specific area induces changes to oscillatory activity that

are synchronous throughout the brain, hence, giving evidence that effects of tDCS are site specific but not site limited [Marshall et al., 2004, 2006]. When we evaluated task against rest conditions, a modulation in synchronization can be appreciated for the θ and α and an even more remarkable change in the high-γ band over the whole brain (notice the change between the first and second columns in Fig. 3). Thus, the observed modulation in synchronization between different brain regions induced by tDCS presented here might be the evidence for tDCS-induced alterations of cortico-cortical and cortico-subcortical network functions mediating the interactions of distant brain regions. Future studies might be of interest to combine transcranial stimulation methods with graph based analysis in visuo-motor and motor coordination focused protocols to achieve a better understanding of the effects of noninvasive cortical stimulation in visuo-motor and motor-coordination networks.

Regarding the effects of tDCS over resting networks (Fig. 3, third column), the stimulation induced a significant synchronization increase within frontal electrodes in the θ, α, and β bands. Moreover, Figure 6 reveals a similar functional topological organization before and after tDCS intervention, with a marked synchronization increase between the frontal electrodes. It is believed that tDCS produces its effects by polarizing brain tissue, where the direction of the polarization depends on the orientation of axons and dendrites in the induced electrical field [Radman et al., 2009; Siebner et al., 2004]. Considering that the frontopolar-placed stimulating electrode was the cathode, it can be speculated whether the negative electric field constantly induced during the 10 min of stimulation might provoke an hyperpolarization of the neurons, therefore, reducing noise within these neural networks and consequently increasing the synchronization of the spontaneous activity over the cathodal stimulated region.

In clinical studies, Stam et al. [2007] describe an EEG functional connectivity loss in patients with AD using graph theory as evaluation approach. On the other hand, application of anodal tDCS enhanced the performance on memory tasks in AD [Boggio et al., 2009]. Furthermore, anodal tDCS over the primary motor cortex contributed to recovery of motor function in stroke patients [Hummel and Cohen, 2005; Hummel et al., 2005]. These results are further supported by reports of improvements in motor function in brain-lesioned rodents and primates [Frost et al., 2003; Plautz et al., 2003; Teskey et al., 2003]. It should be explored in future studies whether tDCS would enhance connectivity and induce synchronization changes in diseases that have been demonstrated to have disrupted networks relative to healthy subjects—such as AD, stroke, and multiple sclerosis [Kotini et al., 2007]—using graph-based analysis as a noninvasive interesting tool to track functional connectivity recovery and to connect these changes with functional improvements.

In conclusion, here we show for the first time that with the application of tDCS, alterations of the cerebral cortex functions can be triggered in terms of changes in brain synchronization and topological functional organization, making it a useful tool to understand brain rhythms, their generation and their topographic specificity. Hence, we propose the use of graph theoretical analysis as a useful tool to noninvasively evaluate not only the functional changes induced by tDCS but also to track the effects of other noninvasive stimulation methods that have also been reported to produce neuroplastic alterations in the human brain (e.g., transcranial random noise stimulation [Terney et al., 2008], transcranial alternating current stimulation [Kanai et al., 2008], and rTMS [Plewnia et al., 2008; Thut and Miniussi, 2009; Thut and Pascual-Leone, 2009, 2010]).

ACKNOWLEDGMENTS

The authors would like to express their gratitude to the Rose Foundation. Their support made possible to conclude this study, which we believe will help us to understand better the effects of tDCS in multiple sclerosis.

REFERENCES

Amunts K, Jaencke L, Mohlberg H, Steinmetz H, Zilles K (2000): Interhemispheric asymetry of the human motor cortex related to handedless and gender. Neuropsychologia 38:304–312.

Antal A, Nitsche MA, Kincses TZ, Kruse W, Hoffmann KP, Paulus W (2004): Facilitation of visuo-motor learning by transcranial direct current stimulation of the motor and extrastriate visual areas in humans. Eur J Neurosci 19:2888–2892.

Boggio PS, Castro LO, Savagim EA, Braite R, Cruz VC, Rocha RR, Rigonatti SP, Silva MT, Fregni F (2006): Enhancement of non-dominant hand motor function by anodal transcranial direct current stimulation. Neurosci Lett 404:232–236.

Boggio PS, Khoury LP, Martins DC, Martins OE, de Macedo EC, Fregni F (2009): Temporal cortex direct current stimulation enhances performance on a visual recognition memory task in Alzheimer disease. J Neurol Neurosurg Psychiatry 80:444–447.

Boros K, Poreisz C, Munchau A, Paulus W, Nitsche MA (2008): Premotor transcranial direct current stimulation (tDCS) affects primary motor excitability in humans. Eur J Neurosci 27:1292–1300.

Breakspear M, Terry JR, Friston KJ, Harris AW, Williams LM, Brown K, Brennan J, Gordon E (2003): A disturbance of nonlinear interdependence in scalp EEG of subjects with first episode schizophrenia. Neuroimage 20:466–478.

Brovelli A, Lachaux JP, Kahane P, Boussaoud D (2005): High gamma frequency oscillatory activity dissociates attention from intention in the human premotor cortex. Neuroimage 28:154–164.

Castro-Alamancos MA, Rigas P (2002): Synchronized oscillations caused by disinhibition in rodent neocortex are generated by recurrent synaptic activity mediated by AMPA receptors. J Physiol 542 (part 2):567–581.

Castro-Alamancos MA, Rigas P, Tawara-Hirata Y (2007): Resonance (~10 Hz) of excitatory networks in motor cortex: Effects of voltage-dependent ion channel blockers. J Physiol 578.1:173–191

Cheyne D, Bells S, Ferrari P, Gaetz W, Bostan AC (2008): Self-paced movements induce high-frequency gamma oscillations in primary motor cortex. Neuroimage 42:332–342.

Cordes D, Haughton VM, Arfanakis K, Wendt GJ, Turski PA, Moritz CH, Quigley MA, Meyerand ME (2000): Mapping functionally related regions of brain with functional connectivity MR imaging. AJNR Am J Neuroradiol 21:1636–1644.

Fox MD, Raichle ME (2007): Spontaneous fluctuations in brain activity observed with functional magnetic resonance imaging. Nat Rev Neurosci 8:700–711.

Frost SB, Barbay S, Friel KM, Plautz EJ, Nudo RJ (2003): Reorganization of remote cortical regions after ischemic brain injury: A potential substrate for stroke recovery. J Neurophysiol 89: 3205–3214.

Hari R, Salmelin R, Makela JP, Salenius S, Helle M (1997): Magnetoencephalographic cortical rhythms. Int J Psychophysiol 26: 51–62.

Hummel F, Cohen LG (2005): Improvement of motor function with noninvasive cortical stimulation in a patient with chronic stroke. Neurorehabil Neural Repair 19:14–19.

Hummel F, Celnik P, Giraux P, Floel A, Wu WH, Gerloff C, Cohen LG (2005): Effects of noninvasive cortical stimulation on skilled motor function in chronic stroke. Brain 128 (Pt 3):490–499.

Kanai R, Chaieb L, Antal A, Walsh V, Paulus W (2008): Frequency-dependent electrical stimulation of the visual cortex. Curr Biol 18:1839–1843.

Klostermann F, Nikulin VV, Kuhn AA, Marzinzik F, Wahl M, Pogosyan A, Kupsch A, Schneider GH, Brown P, Curio G (2007): Task-related differential dynamics of EEG α- and beta-band synchronization in cortico-basal motor structures. Eur J Neurosci 25:1604–1615.

Kotini A, Anninos P, Tamiolakis D, Prassopoulos P (2007): Differentiation of MEG activity in multiple sclerosis patients with the use of nonlinear analysis. J Integr Neurosci 6:233–240.

Lang N, Siebner HR, Ward NS, Lee L, Nitsche MA, Paulus W, Rothwell JC, Lemon RN, Frackowiak RS (2005): How does transcranial DC stimulation of the primary motor cortex alter regional neuronal activity in the human brain? Eur J Neurosci 22:495–504.

Manshanden I, De Munck JC, Simon NR, Lopes da Silva FH (2002): Source localization of MEG sleep spindles and the relation to sources of α band rhythms. Clin Neurophysiol 113: 1937–1947.

Marshall L, Molle M, Hallschmid M, Born J (2004): Transcranial direct current stimulation during sleep improves declarative memory. J Neurosci 24:9985–9992.

Marshall L, Helgadottir H, Molle M, Born J (2006): Boosting slow oscillations during sleep potentiates memory. Nature 444:610–613.

Micheloyannis S, Pachou E, Stam CJ, Breakspear M, Bitsios P, Vourkas M, Erimaki S, Zervakis M (2006): Small-world networks and disturbed functional connectivity in schizophrenia. Schizophr Res 87:60–66.

Montez T, Linkenkaer-Hansen K, van Dijk BW, Stam CJ (2006): Synchronization likelihood with explicit time-frequency priors. Neuroimage 33:1117–1125.

Nitsche MA, Paulus W (2000): Excitability changes induced in the human motor cortex by weak transcranial direct current stimulation. J Physiol 527 Pt 3:633–639.

Nitsche MA, Paulus W (2001): Sustained excitability elevations induced by transcranial DC motor cortex stimulation in humans. Neurology 57:1899–1901.

Nitsche MA, Fricke K, Henschke U, Schlitterlau A, Liebetanz D, Lang N, Henning S, Tergau F, Paulus W (2003a): Pharmacological modulation of cortical excitability shifts induced by transcranial direct current stimulation in humans. J Physiol 553 (part 1):293–301.

Nitsche MA, Liebetanz D, Antal A, Lang N, Tergau F, Paulus W (2003b)Modulation of cortical excitability by weak direct current stimulation—technical, safety and functional aspects. Suppl Clin Neurophysiol 56:255–276.

Nitsche MA, Schauenburg A, Lang N, Liebetanz D, Exner C, Paulus W, Tergau F (2003c)Facilitation of implicit motor learning by weak transcranial direct current stimulation of the primary motor cortex in the human. J Cogn Neurosci 15:619–626.

Nitsche MA, Liebetanz D, Schlitterlau A, Henschke U, Fricke K, Frommann K, Lang N, Henning S, Paulus W, Tergau F (2004): GABAergic modulation of DC stimulation-induced motor cortex excitability shifts in humans. Eur J Neurosci 19:2720–2726.

Oldfield RC (1971): The assessment and analysis of handedness: The Edinburgh inventory. Neuropsychologia 9:97–113.

Omlor W, Patino L, Hepp-Reymond MC, Kristeva R (2007): Gamma-range corticomuscular coherence during dynamic force output. Neuroimage 34:1191–1198.

Plautz EJ, Barbay S, Frost SB, Friel KM, Dancause N, Zoubina EV, Stowe AM, Quaney BM, Nudo RJ (2003): Post-infarct cortical plasticity and behavioral recovery using concurrent cortical stimulation and rehabilitative training: A feasibility study in primates. Neurol Res 25:801–810.

Plewnia C, Rilk AJ, Soekadar SR, Arfeller C, Huber HS, Sauseng P, Hummel F, Gerloff C (2008): Enhancement of long-range EEG coherence by synchronous bifocal transcranial magnetic stimulation. Eur J Neurosci 27:1577–1583.

Radman T, Datta A, Ramos RL, Brumberg JC, Bikson M (2009): One-dimensional representation of a neuron in a uniform electric field. Conf Proc IEEE Eng Med Biol Soc 1:6481–6484.

Salin PA, Bullier J (1995): Corticocortical connections in the visual system: Structure and function. Physiol Rev 75:107–154.

Schoffelen JM, Oostenveld R, Fries P (2005): Neuronal coherence as a mechanism of effective corticospinal interaction. Science 308:111–113.

Siebner HR, Lang N, Rizzo V, Nitsche MA, Paulus W, Lemon RN, Rothwell JC (2004): Preconditioning of low-frequency repetitive transcranial magnetic stimulation with transcranial direct current stimulation: Evidence for homeostatic plasticity in the human motor cortex. J Neurosci 24:3379–3385.

Sporns O, Zwi JD (2004): The small world of the cerebral cortex. Neuroinformatics 2:145–162.

Sporns O, Chialvo DR, Kaiser M, Hilgetag CC (2004): Organization, development and function of complex brain networks. Trends Cogn Sci 8:418–425.

Stam CJ (2005): Nonlinear dynamical analysis of EEG and MEG: Review of an emerging field. Clin Neurophysiol 116:2266–2301.

Montez T, Linkenkaer-Hansen K, van Dijk BW, Stam CJ. (2002): Synchronization likelihood: An unbiased measure of generalized synchronization in multivariate data sets. Phys D 163:236–251.

Stam CJ, Reijneveld JC (2007): Graph theoretical analysis of complex networks in the brain. Nonlinear Biomed Phys 1:3.1–3.9.

Stam CJ, Jones BF, Nolte G, Breakspear M, Scheltens P (2007): Small-world networks and functional connectivity in Alzheimer's disease. Cereb Cortex 17:92–99.

Stam CJ, de Haan W, Daffertshofer A, Jones BF, Manshanden I, van Cappellen van Walsum AM, Montez T, Verbunt JP, de Munck JC, van Dijk BW and others (2009): Graph theoretical analysis of magnetoencephalographic functional connectivity in Alzheimer's disease. Brain 132 (part 1):213–224.

Steriade M, Gloor P, Llinas RR, Lopes de Silva FH, Mesulam MM (1990): Report of IFCN Committee on Basic Mechanisms. Basic mechanisms of cerebral rhythmic activities. Electroencephalogr Clin Neurophysiol 76:481–508.

TeamRDC (2009). R: A Language and Environment for Statistical Computing. R Team: Vienna, Austria.

Tecchio F, Zappasodi F, Porcaro C, Barbati G, Assenza G, Salustri C, Rossini PM (2008): High-gamma band activity of primary hand cortical areas: A sensorimotor feedback efficiency index. Neuroimage 40:256–264.

Terney D, Chaieb L, Moliadze V, Antal A, Paulus W (2008): Increasing human brain excitability by transcranial high-frequency random noise stimulation. J Neurosci 28:14147–14155.

Teskey GC, Flynn C, Goertzen CD, Monfils MH, Young NA (2003): Cortical stimulation improves skilled forelimb use following a focal ischemic infarct in the rat. Neurol Res 25:794–800.

Theiler J (1986): Spurious dimension from correlation algorithms applied to limited time-series data. Phys Rev A 34:2427–2432.

Thut G, Miniussi C (2009): New insights into rhythmic brain activity from TMS-EEG studies. Trends Cogn Sci 13:182–189.

Thut G, Pascual-Leone A (2010): A review of combined TMS-EEG studies to characterize lasting effects of repetitive TMS and assess their usefulness in cognitive and clinical neuroscience. Brain Topogr 22:219–232.

Thut G, Pascual-Leone A (2010): Integrating TMS with EEG: How and what for? Brain Topogr 22:215–218.

Vines BW, Cerruti C, Schlaug G (2008): Dual-hemisphere tDCS facilitates greater improvements for healthy subjects' nondominant hand compared to uni-hemisphere stimulation. BMC Neurosci 9:103.1–103.7.

Waldert S, Preissl H, Demandt E, Braun C, Birbaumer N, Aertsen A, Mehring C (2008): Hand movement direction decoded from MEG and EEG. J Neurosci 28:1000–1008.